

## *Dictyostelium* CBP3 associates with actin cytoskeleton and is related to slug migration

Chang-Hun Lee<sup>a,1,2</sup>, Sun-Young Jeong<sup>a,2</sup>, Beom-Jun Kim<sup>a</sup>, Chang-Hoon Choi<sup>a</sup>, Ji-Sun Kim<sup>a</sup>,  
Byung-Mo Koo<sup>a</sup>, Young-Jae Seok<sup>a</sup>, Hyung-Soon Yim<sup>b,\*</sup>, Sa-Ouk Kang<sup>a,b,\*</sup>

<sup>a</sup>*School of Biological Sciences, Seoul National University, Seoul 151-742, Republic of Korea*

<sup>b</sup>*Institute of Microbiology, Seoul National University, Seoul 151-742, Republic of Korea*

Received 6 July 2004; received in revised form 24 December 2004; accepted 4 January 2005

Available online 29 January 2005

### Abstract

Calcium-binding protein 3 (CBP3) expression was up-regulated under the control of the actin 15 promoter and down-regulated by RNA interference in *Dictyostelium discoideum*. The overexpression of CBP3 accelerated cell aggregation and formed small aggregates and fruiting body. CBP3-inhibited cells showed uneven aggregation and increased slug trail lengths toward the directed light, whereas CBP3-overexpressing cells showed the opposite phenomena. Under dark condition, the enhanced slug trail length was also observed in the CBP3-inhibited cells. Yeast two-hybrid screening identified actin 8 as interacting protein with CBP3. The interaction between CBP3 and actin was confirmed by  $\beta$ -galactosidase assay and surface plasmon resonance. CBP3 was associated with Triton X-100-insoluble cytoskeleton in the presence of  $\text{Ca}^{2+}$  and the interaction of CBP3 with cytoskeleton was increased by the addition of  $\text{Ca}^{2+}$ . Using fluorescence microscopy, CBP3 was also shown to associate with the actin cytoskeleton during development. Subcellular fractionation indicated that CBP3 was enriched in cytosolic fraction. Taken together, these results suggest that CBP3 interacts with actin cytoskeleton and has a role during cell aggregation and slug migration of *Dictyostelium*.

© 2005 Elsevier B.V. All rights reserved.

**Keywords:** Calcium-binding protein 3; Actin cytoskeleton; Slug migration; *Dictyostelium discoideum*

### 1. Introduction

Calcium ions ( $\text{Ca}^{2+}$ ) are the important signaling ions within cells and regulate diverse cellular processes in both higher and lower eukaryotes [1,2]. Many cellular functions are directly or indirectly regulated by the free cytosolic  $\text{Ca}^{2+}$  concentration ( $[\text{Ca}^{2+}]_i$ ) and intracellular  $\text{Ca}^{2+}$  levels are monitored by a variety of  $\text{Ca}^{2+}$ -binding proteins [3]. These proteins function as  $\text{Ca}^{2+}$  buffers or  $\text{Ca}^{2+}$  transporters, which do not undergo a significant change in conformation on

$\text{Ca}^{2+}$  binding or as  $\text{Ca}^{2+}$  sensors that undergo a  $\text{Ca}^{2+}$ -induced conformational change [4]. Many of these calcium-binding proteins are supposed to work as  $\text{Ca}^{2+}$  sensors that detect intracellular calcium concentration change and transduce  $\text{Ca}^{2+}$  signals to downstream effector molecules and regulatory pathways.

*Dictyostelium discoideum* is a unicellular amoeba that feeds on bacteria. When food becomes depleted, the amoebae enter a developmental stage, leading to the formation of a multicellular organism (slug) and finally to a fruiting body, which consists of stalk and spore cells. When the spores meet the appropriate environmental conditions, spores can germinate and give rise to amoebae, which completes the life cycle [5]. The role of calcium ion in the regulation of the development of *Dictyostelium* is being widely studied. Many lines of evidence suggested that  $\text{Ca}^{2+}$  ion is involved in numerous developmental processes,

\* Corresponding authors. Fax: +82 2 888 4911.

E-mail addresses: [wuseok@hotmail.com](mailto:wuseok@hotmail.com) (H.-S. Yim), [kangsaou@snu.ac.kr](mailto:kangsaou@snu.ac.kr) (S.-O. Kang).

<sup>1</sup> Present address: Cancer Research Institute, Catholic University, Seoul 137-701, Republic of Korea.

<sup>2</sup> These authors equally contributed to this work.

such as chemotaxis [6–8], cell–cell adhesion [9], cell fate determination [10–13], and starvation signals transduction [14].

Until now, thirteen different genes encoding small  $\text{Ca}^{2+}$ -binding proteins have been identified in *Dictyostelium*. *calA* which encodes calmodulin [15] and *calB* which encodes calmodulin-like protein [16] are expressed in both vegetative and developing cells. *cafA* (calfumirin) is expressed preferentially at the initial stage of differentiation [17] and overexpression of the *cafA* protein (CAF1) has a stimulatory effect on differentiation [18]. *cbpA* (CBP1) is expressed preferentially during the multicellular stages of development [19]. CBP1 associates with cytoskeleton and the disruption of *cbpA* results in impairments of aggregation under certain developmental conditions [20]. The mRNA level of *cbpB* was significantly increased during the development, but its role was unknown [21]. *cbpC* (CBP3) mRNA was expressed at early developmental stage and disappeared after 12 h of the development, but the protein level was maintained thereafter [22]. CBP4a (*cbpD1*) and CBP4b (*cbpD2*) were identified as binding proteins to CBP1 in yeast two-hybrid screening using the CBP1 as a bait [23]. Recently, by yeast two-hybrid screening, CBP4a was also identified as an interacting protein of nucleomorphin, which is a nuclear calmodulin-binding protein [24]. *cbpE*, *cbpF*, *cbpG*, *cbpH*, and *cbpI* are only known as cDNA or genomic DNA sequences. The protein products of these genes have similar properties in that they have small sizes of about 20 kDa and the sequences of EF-hand domains and their relative positions in primary structures are almost the same. In spite of their common properties, they exhibit very low amino acid sequence identity (except in their EF-hands), several specific features in their amino acid compositions, differences in affinity for  $\text{Ca}^{2+}$ , and different expression patterns. These suggest that each calcium-binding protein might have a function to regulate specific  $\text{Ca}^{2+}$ -dependant processes in development.

To assess the function of CBP3 during development, *cbpC*-overexpressing and *cbpC*-inhibited strains were obtained and their developmental phenotypes were compared. Yeast two-hybrid screening [25] was carried out to identify its interacting partners and in vivo and in vitro localization of CBP3 were performed.

## 2. Materials and methods

### 2.1. Culture conditions, transformation and development

The axenic parental strain KAx3 cells were grown in HL5 medium according to Cocucci and Sussman [26], which was supplemented with 200  $\mu\text{g}$  of streptomycin sulfate/ml and 200 unit of penicillin/ml, shaken 150 rpm at 22 °C. For transformants, HL5 medium supplemented with 20  $\mu\text{g}/\text{ml}$  of G418 was used. *Dictyostelium* transformation was performed according to the protocol [27] with some

modifications [28]. Synchronous development of cells was induced by collecting exponentially growing cells ( $2\text{--}5\times 10^6/\text{ml}$ ), washing them with the development buffer (DB; 5 mM phosphate buffer, pH 6.1), and depositing them at a density of  $1\text{--}2\times 10^6/\text{cm}^2$  on nitrocellulose filters or non-nutrient agar plate (DB agar plate) and incubating at 22 °C. For submerged development, the washed cells were developed on plate under DB.

### 2.2. Plasmid construction and molecular biology

The expression vector for the CBP3 protein in *Dictyostelium* was constructed by polymerase chain reaction (PCR), using pET-CBP3 [22] as a template and P1 (5'-TTTATGATCTTATATGTTAACTAAT-3') and P2 (5'-CTCGAGTTTTTTTAAACAATGT-3') as primers. The PCR product was cloned into pGEM-T easy vector (Promega) and cut by *Bgl*II and *Spe*I. The resulting fragment was ligated into EXP-4(+) (kindly provided by Dr. R.A. Firtel) yielding CBP3-EXP. For making RNA interference construct, short 5'-fragment was synthesized using primer P1 and P3 (5'-CTCATAAGAATTGCCATTC-3') and cloned into pGEM-T easy vector. The plasmid that had a sense orientation was digested with *Spe*I and the overhangs were blunt-ended by Klenow fragment (Promega), followed by digestion with *Bgl*II. The full-length CBP3 fragment that had a sense orientation was also digested with *Spe*I and overhangs were blunt-ended by Klenow fragment (Promega), followed by digestion with *Eco*RI. These one end blunt-ended short 5'-fragment and full-length fragments were ligated altogether into the *Bgl*II and *Eco*RI sites of the EXP-4(+) vector to express fold-back orientation RNA transcripts. The *Bgl*II and *Xho*I fragment of CBP3-EXP was ligated into pTX-GFP vector (kindly provided by Dr. Egelhoff) for the construction of green fluorescent protein (GFP) fusion protein with CBP3. For yeast two-hybrid screening, the full-length CBP3 coding region was amplified using PCR and cloned into the Gal4 DNA-binding domain vectors pGBDU (kindly provided by Dr. James) [29] and pGBT9 (Clontech), yielding pGBDU-CBP3 and pGBT9-CBP3, respectively.  $\gamma$ -Glutamylcysteine synthetase (GCS) cDNA from *Dictyostelium* was amplified using PCR and cloned in-frame into pACT2 vector. The resultant vector, pACT2-GCS, was used as a negative control plasmid for  $\beta$ -galactosidase assay.

### 2.3. Yeast two-hybrid analysis

The Gal4 yeast two-hybrid system was used to detect protein–protein interactions. The yeast strain PJ69-4A (kindly provided by Dr. P. James), which carries the *HIS3*, *ADE3*, and *lacZ* reporter genes under the control of Gal4-responsive elements [29], was used for library screening. The *Dictyostelium* cDNA library (kindly provided by Dr. S. Lu) was cloned into the *Eco*RI/*Xho*I sites of the Gal4 activation domain (AD) vector pACT2. The library was

constructed from a mixture of mRNAs isolated from cells under development between 4 and 18 h. PJ69-4A harboring pGBDU-CBP3 was sequentially transformed with the cDNA library by the lithium acetate/single-stranded DNA/polyethylene glycol method [30]. Transformants were selected in minimal medium lacking Ura, Leu, Ade, and His. AD plasmids were isolated from positive clones according to the protocol [31]. The isolated AD plasmids were rescued by the complementation of the *leuB6* deficiency in the *E. coli* strain HB101 and prepared from the HB101 growers and further tested for specificity by cotransformation into PJ69-4A with pGBDU-CBP3 or with pGBDU. The AD plasmids recovered from positive clones were sequenced. The AD plasmid or pACT2 alone and pGBT9-CBP3 or pGBT9 alone were cotransformed into yeast strain Y190 and assayed for  $\beta$ -galactosidase activity as described [32]. pACT2-GCS was used as a negative control for CBP3 interaction.

#### 2.4. Purification of actin

The cytoskeleton isolated from vegetative cells was used as the starting material for *Dictyostelium* actin preparation. Cytoskeleton was prepared as described previously [33]. The actin associated with the cytoskeleton can be dissociated by depolymerization at low ionic strength. The cytoskeleton pellet was resuspended into 2 volumes of depolymerizing buffer (10 mM triethanolamine, pH 8.0, 0.5 mM ATP, 0.5 mM dithiothreitol (DTT), and 20  $\mu$ M  $MgCl_2$ ) per gram of the starting cell pellet. The resuspended cytoskeleton was dialyzed against 100 volumes of depolymerizing buffer. After dialysis, the preparation was centrifuged at 100,000 $\times g$  for 2 h to recover the solubilized actin. The solubilized actin was further purified using Resource Q, ion exchange chromatography column (Pharmacia) equilibrated with depolymerizing buffer.

#### 2.5. Overexpression of recombinant CBP3 protein and purification

*E. coli* BL21 (DE3) pLysS cells harboring pET-CBP3 was grown in an LB medium containing ampicillin. Cells were grown to  $OD_{600}$  of 0.5 at 37 °C and expression was induced by 1 mM isopropyl- $\beta$ -D-thiogalactopyranoside (IPTG). After a 3 h induction, the cells were collected and stored at –20 °C. The frozen cells were thawed and suspended in a binding buffer (5 mM imidazole, 0.5 M NaCl, 20 mM Tris–HCl, pH 7.9) and were gently sonicated and centrifuged at 12,000 rpm for 15 min. The pellets were solubilized in a binding buffer, which contained 6 M urea and purified using Ni-affinity column under the denaturation condition (Novagen). The eluents were strongly reduced by adding DTT to a final concentration of 20 mM and refolded rapidly by 100-fold dilution into a refolding buffer (20 mM Tris–HCl, pH 8.5, 30 mM L-arginine, 0.5 mM oxidized glutathione, 150 mM NaCl, 2.5 mM  $CaCl_2$ ). The concen-

tration of the protein during the refolding process was approximately 10  $\mu$ M. The samples were incubated at room temperature for 2 h and concentrated by ultrafiltration (Amicon). The N-terminal His-tag leader was removed by thrombin protease. The cleavage of the His-tag leader and the purity of the protein were assessed by sodium dodecylsulfate-polyacrylamide gel electrophoresis (SDS-PAGE). The concentration of the protein was measured using  $D_C$  protein assay kit (Bio-Rad).

#### 2.6. Measurement of surface plasmon resonance (SPR)

The interaction of CBP3 with actin was monitored using a SPR biosensor instrument, BIAcore-3000 (BIAcore AB). CBP3 was immobilized on the carboxymethylated dextran surface of a CM5 sensor chip by amine coupling according to the manufacturer's instructions (BIAcore AB). The carboxymethylated dextran matrix was activated by mixing equal volumes of 0.1 M *N*-hydroxysuccinimide (NHS) and 0.4 M *N*-ethyl-*N*-(dimethyl-aminopropyl) carbodiimide hydrochloride and injecting 50  $\mu$ l mixture over the sensor chip surface at a flow rate of 5  $\mu$ l/min. CBP3 was diluted to 100  $\mu$ g/ml in 50  $\mu$ l coupling buffer (10 mM sodium acetate, pH 4.5) and injected at a flow rate of 5  $\mu$ l/min over a sensor chip. Unreacted NHS was inactivated by injecting 40  $\mu$ l of 1 M ethanolamine–HCl, pH 8.0. Actin was diluted to 30  $\mu$ g/ml in running buffer containing 10 mM *N*-[2-hydroxyethyl]piperazine-*N'*-[2-ethanesulfonic acid] (HEPES), pH 7.5, 150 mM NaCl, 1 mM DTT, and 5 mM  $CaCl_2$  or 5 mM ethylene glycol-bis( $\beta$ -aminoethylether)-*N,N,N',N'*-tetraacetic acid (EGTA). The flow rate during the experiments was 10  $\mu$ l/min. The regeneration was performed with 5  $\mu$ l of 2 M NaCl. The curve corresponding to the difference between binding to CBP3 and a blank chip was used for analysis. 1000 resonance units correspond to a surface density of 1 ng/mm<sup>2</sup>.

#### 2.7. SDS-PAGE and immunoblot analysis

SDS-PAGE was performed according to the protocol [34]. After electrophoresis, the gel was stained with Coomassie Blue R-250. For immunoblot analysis, SDS-PAGE was performed on 15% polyacrylamide slab gel. The electrotransfer of proteins from the gel to the nitrocellulose membrane (0.45  $\mu$ m pore size; MBI Fermentas) was carried out according to the method [35]. The transferred membrane was blocked by Tris-buffered saline (TBS; 10 mM Tris–HCl, pH 7.5, containing 150 mM NaCl) containing 1% bovine serum albumin (BSA) and 0.02% sodium azide. This membrane was then incubated in TBST (TBS containing 0.05% Tween 20) containing 1:10000-diluted anti-CBP3 antiserum (from mouse) [22] overnight at room temperature. After washing for 15 min with three changes of TBST, the membrane was incubated for 90 min with 1:10000 diluted alkaline phosphatase conjugated anti-mouse IgG antibody (Roche applied science). The membrane was then washed

for 15 min with three changes of TBST and rinsed with alkaline phosphatase buffer (100 mM Tris–HCl, pH 9.5, 100 mM NaCl, 10 mM MgCl<sub>2</sub>). For color development, the membrane was incubated in 20 ml of alkaline phosphatase buffer containing 8 mg of 5-bromo-4-chloro-3-indoyl phosphate and 16 mg of nitro blue tetrazolium at 37 °C.

### 2.8. RNA extraction and Northern blot analysis

*Dictyostelium* amoebae were developed on nitrocellulose filters for 6 h and were taken for RNA extraction. Total RNA was isolated using TRIzol reagent according to the supplier's recommendations (Gibco BRL). For Northern blot analysis, 20 µg samples of total RNA were separated on 1% agarose gel containing 0.22 M formaldehyde and transferred to Hybond-N+ membrane filter (Amersham Pharmacia Biotech). The coding region of *cbpC* was generated by PCR and labeled with [ $\alpha$ -<sup>32</sup>P]-dATP by random priming. The blot was prehybridized for 1 h, hybridized for 2 h and washed twice for 20 min at 65 °C. The signal was visualized by exposing the membrane to X-ray film.

### 2.9. Fluorescence microscopy

Cells were developed on coverslips or DB plates for different time periods and then fixed with 3.7% formaldehyde in 17 mM phosphate buffer, pH 6.5, for 15 min at room temperature, followed by permeabilization with cold methanol (–20 °C) containing 1% formaldehyde for 5 min. Nonspecific binding was blocked by incubation with 1% (w/v) BSA in the phosphate-buffered saline (PBS; 6 mM Na<sub>2</sub>HPO<sub>4</sub>/KH<sub>2</sub>PO<sub>4</sub>, pH 6.9, containing 130 mM NaCl) for 10 min. Samples were incubated with the anti-CBP3 antiserum (1:200 dilution in PBS containing 0.1% BSA) for 1 h, washed three times with PBS containing 0.05% Tween-20, and then stained with fluorescein isothiocyanate (FITC)-conjugated goat anti-mouse IgG (1:300 dilution) for 1 h. For F-actin cytoskeleton labeling, tetramethylrhodamine-5-isothiocyanate (TRITC)-labelled phalloidin was used. Coverslips were mounted in PBS containing 80% glycerol, 0.2% *p*-phenylenediamine, and 2.5% 1,4-diazabicyclo-[2,2,2]-octane [36]. Images were acquired using an Axiovert 100 inverted microscope equipped with a 32× Neofluar objective (Carl Zeiss). When the GFP fusion protein expressed strain was used, cells were developed on DB-plate and live images were obtained.

### 2.10. Isolation of detergent-insoluble cytoskeleton and cell fractionation

Triton X-100-insoluble cytoskeleton was isolated from vegetative and developed cells as described [20]. Briefly, cells (1–10×10<sup>7</sup>) were washed and resuspended in 300 µl of ice-cold 20 mM MES–NaOH, pH 6.6, and were added to 1.0 ml of cold E buffer (80 mM PIPES–NaOH, 5 mM EGTA, 5

mM MgCl<sub>2</sub>, 0.5 mM dithiothreitol, 30% glycerol, 1% Triton X-100, 1 mM phenylmethylsulfonyl fluoride, 10 µl of protease inhibitor cocktail, pH 6.8). In some experiments, this buffer was modified by replacing the EGTA with 5 mM CaCl<sub>2</sub> (C buffer) or 5 mM MgCl<sub>2</sub> (M buffer). The collected cells were lysed by inverting several times at room temperature and the insoluble material was collected by centrifugation at 10,000×*g* for 5 min at 4 °C. The pellets were washed one or more times in 1 ml of E or C buffer without detergent. Finally, the pellets were resuspended in 50–100 µl of phosphate buffer and frozen at –80 °C before use. Subcellular fractionation was carried out according to the protocol [37].

### 2.11. Phototaxis assay

Phototaxis experiments were performed as described [38]. KAx3 or mutant cells were applied to the surface of a DB-agar plate or a charcoal-agar plate (9 cm in diameter) to give a density of 1×10<sup>6</sup> cells/cm<sup>2</sup>. The application point was asymmetrically located to one side of the plate and its distance to the light port was 10 cm. In control experiments conducted in the absence of light, cells were applied to the center of the plate. After incubation for 48 h at 22 °C in a phototactic chamber, the distances of slug migration from the center of the initial cell deposit were photographed and migration distance was measured.

## 3. Results

### 3.1. Overexpression and RNA interference of CBP3 in *D. discoideum*

We have previously showed the cloning and characterization of *cbpC* from *D. discoideum* [19]. To investigate its role, *cbpC* was cloned into EXP-4(+) and overexpressed in *D. discoideum*. One of the cell lines overexpressing CBP3, clone 10, was named CHE10 and chosen for further experiments. The immunoblot analysis of CHE10 and KAx3 (parental axenic strain) cell crude extracts after 12 h development indicates that CBP3 was overexpressed successfully in CHE10 (Fig. 1A, lanes 1 and 2). Although considerable effort has been made to disrupt the *cbpC* gene, no knockout mutant of CBP3 was obtained. Using antisense mRNA constructs, we also failed to select stable cell lines with a reduced expression level of CBP3. Recently, RNA interference mechanism proved to be working in *Dictyostelium* [39]. So, we applied this method to silence the *cbpC* gene. To express fold-back RNA in *Dictyostelium*, the 5'-130 bp-fragment of *cbpC* and the full open reading frame of *cbpC* gene were ligated into EXP-4 (+) and transformed into KAx3 cells. Immunoblot analysis showed that the level of CBP3 was reduced about 80 to 90% in the RNAi cells compared to the KAx3 cells. Clone 2 of these RNAi cell lines was named CHI2 and used for further experiments

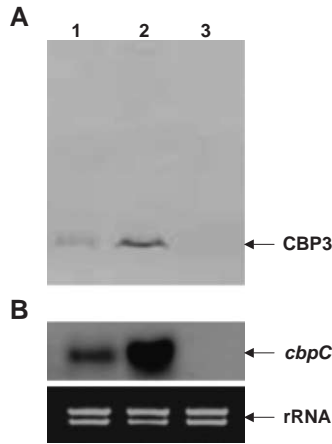


Fig. 1. The expression of CBP3 protein (A) and mRNA (B) in KAx3, CHE10, and CHI2 strains. Lane 1, KAx3 cells; lane 2, CHE10 cells; and lane 3, CHI2 cells. (A) *Dictyostelium* cells were developed for 12 h on DB plates and harvested. After cell lysis, equal amounts of proteins were analyzed by SDS-PAGE and immunoblotted with anti-CBP3 antibody. (B) Total RNA was isolated from cells developed for 6 h and hybridized with probe for *cbpC*. rRNA was shown as a loading control.

(Fig. 1A, lane 3). Northern blot analysis of CHE10 and CHI2 indicated that the mRNA level of these strains were also up- or down-regulated compared to parental strain KAx3 (Fig. 1B).

### 3.2. Developmental phenotypes and slug migration

Each strain was developed on nitrocellulose filters containing a development buffer and developmental timing and morphology were monitored. During the development, starving KAx3 cells showed the normal developmental timing and morphogenesis. CHE10 cells formed an aggregate center about 1 to 2 h earlier than KAx3 cells and the resulting aggregates were small in size but large in number and resulting fruiting bodies were also smaller than KAx3 cells. While KAx3 cells aggregates elongated and formed finger and migrating slug formed by 12 h, large proportions of CHE10 cells remained in tight aggregates. After 12 h, CHE10 cells showed similar developmental timing and morphologies to KAx3 cells. In CHI2 cells, aggregation timing was similar to that of KAx3 cells, but some of the cells remained in the substratum. The resulting aggregates were a little bigger than KAx3 cells and varied in size. The developmental timing and morphogenesis of CHI2 cells were similar to KAx3 cells (data not shown).

To see the effect of CBP3 overexpression on aggregate number, cells at a density of  $1.0 \times 10^6$  cells/cm<sup>2</sup> were developed at 22 °C for 10 h and the number of aggregates was scored (Table 1). From the statistical analysis using the Minitab program (Minitab Inc.), CHE10 cells formed 2.6-fold more aggregates than KAx3 cells ( $P$  value <0.05), but the resulting aggregates were small in size. The number of CHI2 aggregates was somewhat smaller than for KAx3, but this difference was not statistically significant ( $P$  value

Table 1

Aggregate numbers of KAx3, CHE10, and CHI2 strains

Numbers of aggregates			Fold increase		
KAx3	CHE10	CHI2	KAx3	CHE10	CHI2
141±4.58	368±35.6	126±12.5	1	2.6	0.89

Cells were plated at a density of  $1.0 \times 10^6$  cells/cm<sup>2</sup> and permitted to develop at 22 °C for 10 h, and then the numbers of aggregates were scored. The numbers are the means±standard deviations for three different plates. During the development, starving KAx3 cells showed the normal developmental timing and morphogenesis.

>0.05). To verify the differences in developmental timing between strains, Northern blot analysis was carried out for several developmental marker genes, but there were no differences between strains (data not shown).

*Dictyostelium* slugs can sense light and temperature and migrate toward them [40]. In the phototaxis assay (Fig. 2A), each strain showed a different distance of slug migration. KAx3 slugs migrated to the light and the migration distance was ranging from 0.5 to 2 cm ( $1.28 \pm 0.41$  cm) from the deposit center. A few slugs migrated farther than 2 cm. CHE10 slugs migrated ranging from 0.5 to 1 cm ( $0.64 \pm 0.11$  cm) and the number of tractable slugs was very few. In contrast, CHI2 slugs migrated farther than KAx3, ranging from 0.5 to 3.5 cm ( $1.84 \pm 0.82$  cm) (Fig. 3). From the statistical analysis, CHE10 and CHI2 had statistically meaningful migration distance to KAx3 ( $P$  value <0.05). Under the dark condition, KAx3 or mutant cells were applied to the center of a DB-agar plate to give a density of  $1 \times 10^6$  cells/cm<sup>2</sup>. After incubation for 48 h at 22 °C in a phototactic chamber, the distances of slug migration from the center of the initial cell deposit was measured (Fig. 2B). The slug numbers were scored when the slug reached

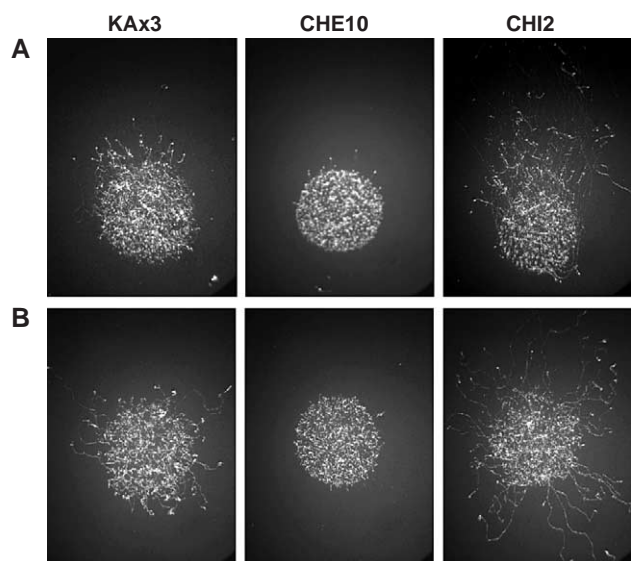


Fig. 2. Phototaxis of KAx3, CHE10, and CHI2 strains. Each *Dictyostelium* cells were developed on DB plate for 48 h under unidirectional light (A) (the light was on the upper side of the figure) or in the dark (B) and photographed.

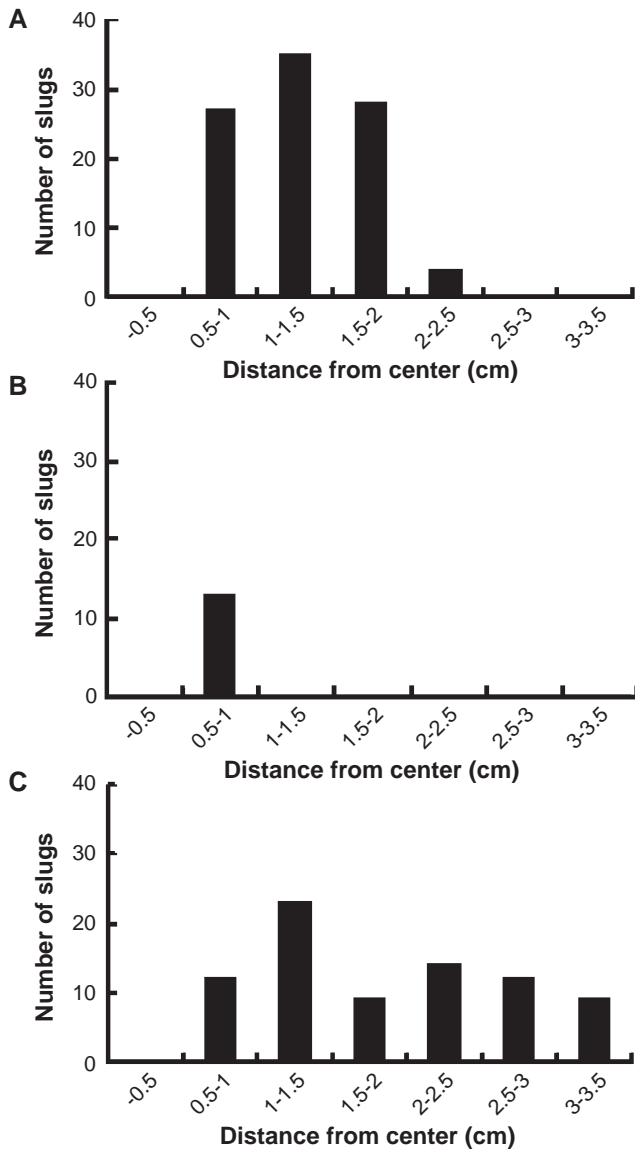


Fig. 3. The distance of slug movement and numbers of slugs migrated to the direction of the light. Each strain was developed under the directed light. After 40 h, migrating slugs were counted and the migrating distance from the cell deposit center was measured. The data were sum of three independent plates. (A) KAx3, (B) CHE10, and (C) CHI2 strains.

further the outside territory of the initial deposit (about 0.5 cm). Distance and slug numbers are the means  $\pm$  standard deviations for the three different plates. KAx3 slugs migrated outward and migration distance was about 2.2 (2.13  $\pm$  0.3 cm). The number of migrated slugs was about 22 (21.7  $\pm$  2.6). The migration distance of CHI2 slugs was about 2.0 cm (2.0  $\pm$  0.2 cm) and slug numbers were 22, similar to KAx3, while CHE10 showed only 4 tractable slugs and migration distance was about 0.7 cm (0.7  $\pm$  0.1 cm). The slug migration distance among KAx3, CHE10 and CHI2 also showed statistically meaningful difference ( $P$  value  $<$  0.05). From these results, we suggested that CBP3 expression was involved in slug trail lengths and this role was not influenced by light.

### 3.3. Identification of actin as binding partner for CBP3 by yeast two-hybrid screening

In order to identify the cellular interaction partners of the CBP3 protein, yeast two-hybrid screening was carried out. The yeast strain PJ694-A containing a bait plasmid pGBDU-CBP3 was transformed with a *Dictyostelium* cDNA library in the pACT2 vector. From about  $1.0 \times 10^7$  transformants, one strongly positive clone was identified. The sequencing analysis of the plasmid isolated from positive clone revealed that the cDNA insert encoded the actin 8. To confirm the positive interaction, we performed two-hybrid assays in the presence and absence of CBP3 and  $\gamma$ -glutamylcysteine synthetase (GCS) as a negative interaction protein for CBP3. Since the pACT2 plasmid did not autonomously activate reporter gene expression, positive protein interaction was only observed in the yeast into which both the CBP3 and isolated library plasmid were co-transformed (Fig. 4A). Furthermore, the interaction of CBP3 and actin was quantified using liquid  $\beta$ -galactosidase assay. From three independent experiments, CBP3 and actin

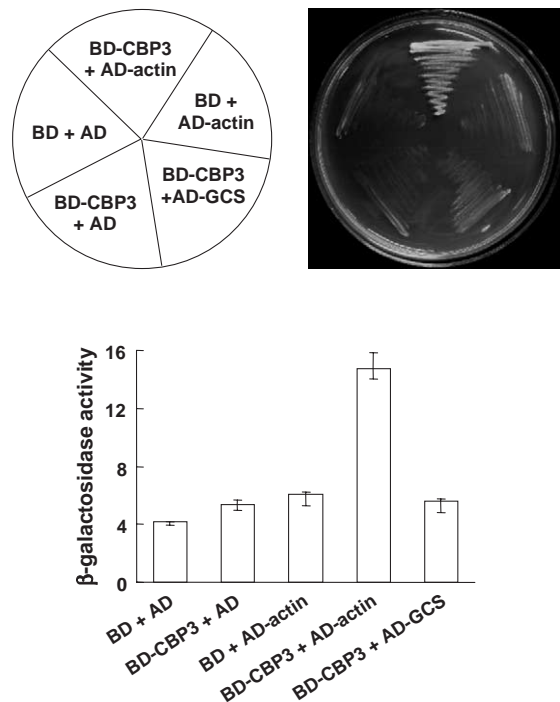


Fig. 4. Yeast two-hybrid analyses of the interaction of CBP3 and actin. (A) Growth of transformed yeast on selective plates. Yeast strain Y190 was cotransformed with the indicated constructs (left). CBP3 coding region was fused in-frame to the Gal4 DNA binding domain in pGBT9 (BD-CBP3) and actin gene rescued from cDNA library was fused to the Gal4 activation domain in pACT2 (AD-actin). BD-CBP3 and AD-actin were cotransformed into yeast Y190 cells. pACT2 (AD), pGBT9 (BD), and pACT2 with GCS (AD-GCS) were used as negative controls. Transformed Y190 cells containing both plasmids were streaked out on the plates lacking adenine, histidine, leucine, and tryptophan (SD/-Ade/-His/-Leu/-Trp). (B) Liquid  $\beta$ -galactosidase activity of transformed yeast. The values were the averages of three independent experiments.

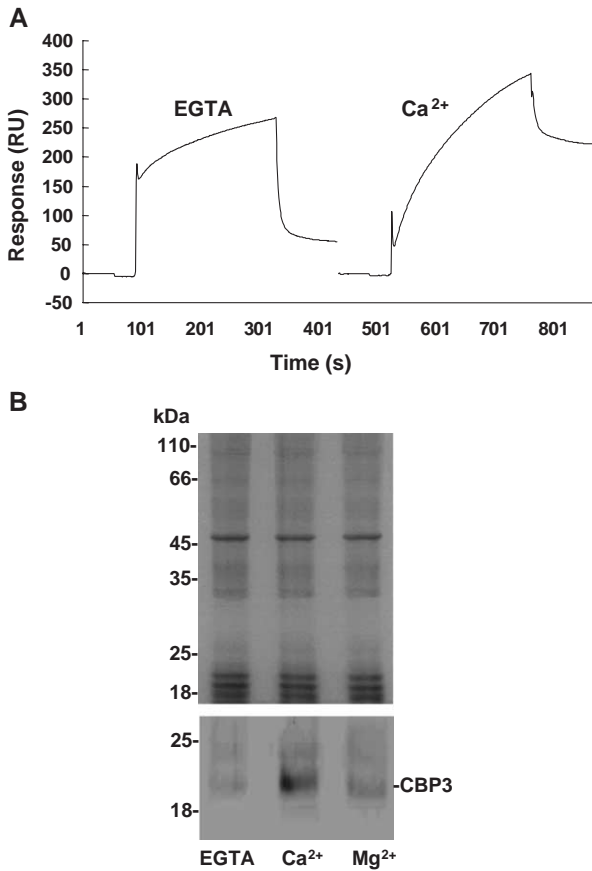


Fig. 5.  $\text{Ca}^{2+}$ -enhanced interaction between CBP3 and actin. (A) Real time interaction analysis of actin with immobilized CBP3. Direct interaction between CBP3 and actin was measured by changes in SPR signal. Purified recombinant CBP3 was immobilized on the surface of a CM5 sensor chip as described in Materials and methods. Purified actin was allowed to flow over the CBP3 surface in the presence of 5 mM EGTA or 5 mM  $\text{Ca}^{2+}$ . (B) Effect of  $\text{Ca}^{2+}$  on CBP3 binding to the cytoskeleton. Triton X-100 insoluble fraction was prepared in the presence of 5 mM EGTA, 5 mM  $\text{Ca}^{2+}$ , and 5 mM  $\text{Mg}^{2+}$ , respectively. The prepared fractions were stained with Coomassie brilliant R-250 (upper panel) and immunoblotted with anti-CBP3 antibody (lower panel). Molecular mass markers in kilodaltons (kDa) are shown at the left of each panel.

showed statistically meaningful interaction compared to other controls ( $P$  value  $<0.05$ ) (Fig. 4B).

### 3.4. $\text{Ca}^{2+}$ enhances the interaction of CBP3 with actin

The interaction of CBP3 and actin was monitored by SPR detection using the BIAcore 3000 system (BIAcore AB). SPR detects a change in refractive index resulting from the interaction of a soluble protein with another protein adsorbed to a surface [41]. Calmodulin and troponin C, well-known EF-hand proteins, undergo  $\text{Ca}^{2+}$ -induced conformational changes to activate their downstream targets [42]. Accordingly, SPR analysis was used to measure the extent of interaction of CBP3 and actin in the presence and absence of calcium ion. For SPR studies, recombinant CBP3 was prepared and immobilized to the surface of a CM5 chip and actin purified from *Dictyostelium* was passed over the

CBP3-immobilized chip in the presence of 5 mM  $\text{Ca}^{2+}$  or 5 mM EGTA. CBP3 had about 3 times higher affinity toward actin in the presence of  $\text{Ca}^{2+}$  than in the absence of  $\text{Ca}^{2+}$  (Fig. 5A). These results demonstrated that CBP3 interacted with actin directly and  $\text{Ca}^{2+}$  enhanced this interaction.

To confirm the effect of  $\text{Ca}^{2+}$  on the CBP3–actin interaction, Triton X-100-insoluble fractions, enriched with actin cytoskeleton, were prepared and analyzed by SDS-PAGE and immunoblot with anti-CBP3 antibody. The actin cytoskeleton contents prepared in the presence of EGTA,  $\text{Ca}^{2+}$ , and  $\text{Mg}^{2+}$  were almost same (Fig. 5B, upper panel), but the associated CBP3 content was high in  $\text{Ca}^{2+}$ -added

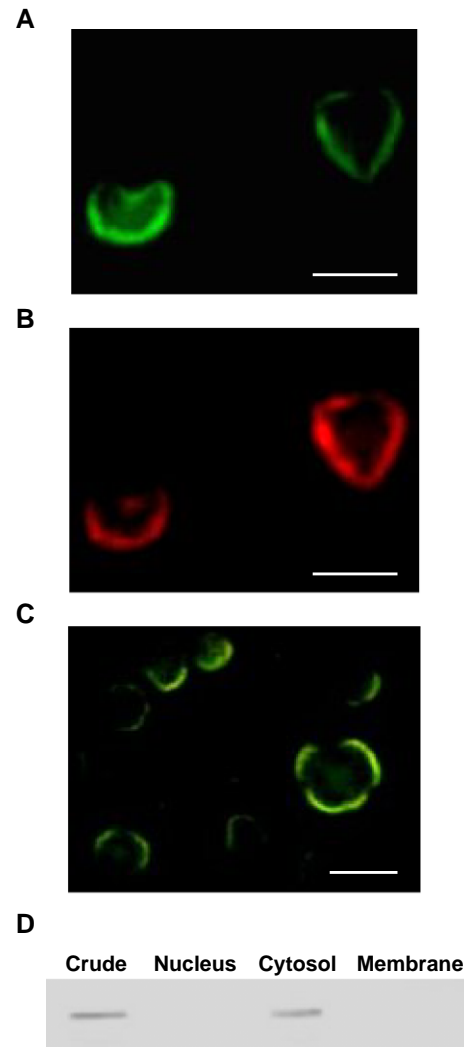


Fig. 6. In vivo and subcellular localization of CBP3. KAX3 cells were developed for 10 h on the coated cover slide and images were obtained by Axiovert 100 microscope. Cells were fixed and stained with anti-CBP3 antibody and FITC-conjugated anti-IgG antibody and TRITC-phalloidin. Images were obtained using fluorescence reflector equipped with blue-violet (A) or green excitation filter (B). (C) When GFP was fused with CBP3, cells were developed for 10 h and live images were captured. Bar indicates 10  $\mu\text{m}$ . (D) Subcellular localization of CBP3. KAX3 cells were developed for 10 h and their nucleus, cytosol, and membrane fractions were prepared by differential centrifugation and immunoblotted with anti-CBP3 antibody.

preparation compared to the other preparations (Fig. 5B, lower panel). This suggests that CBP3 associated with actin cytoskeleton and this association was increased in the presence of  $\text{Ca}^{2+}$ .

### 3.5. Intracellular and subcellular localization of CBP3

For the cellular localization of CBP3, KAx3 cells were developed under the DB for 10 h and transferred to cover slide. After fixing and permeabilization, cells were stained with anti-CBP3 antibody and FITC-labeled anti-mouse IgG antibody and TRITC-labelled phalloidin. The resultant images showed that CBP3 was somewhat diffusely distributed in the cytoplasm and concentrated in the cortical region or membrane (Fig. 6A). The F-actin exhibited the same distribution with CBP3 (Fig. 6B). These results support the finding that CBP3 interacts with actin in *Dictyostelium*. Cells expressing GFP-tagged CBP3 (Fig. 6C) also showed a similar distribution as native CBP3 (Fig. 6A).

To examine further the subcellular distribution of CBP3, KAx3 cells developed for 10 h were separated into nuclear, membrane, and cytosolic fraction by differential centrifugation and analyzed by immunoblot with anti-CBP3 antibody. As shown in Fig. 6D, CBP3 was highly enriched in the cytosolic fraction not in nuclear and membrane fractions. These results indicated that while CBP3 was concentrated in the cell cortex, CBP3 was localized in cytoplasmic region.

## 4. Discussion

To assess the role of CBP3 during development, CBP3 was overexpressed and its expression level was inhibited by RNA interference. Double-stranded RNA (dsRNA) mediated RNA interference has been applied efficiently to *Dictyostelium* [39]. In the case of *cbpC*, RNA interference method inhibited its expression level efficiently (Fig. 1). When CBP3-overexpressing cells, CHE10, were plated on DB agar plate at standard densities, they had a tendency to aggregate faster than parental KAx3 cells. Northern blot analysis for several developmental marker genes showed that there was no difference between strains (data not shown), indicating that the effect of CBP3 on the developmental morphology is not serious.

When the distance of slug migration was compared, each strain showed different slug trail length. CBP3-overexpressing cells, CHE10, showed reduced slug migration, while CBP3-inhibited cells, CHI2, enhanced slug migration (Figs. 2 and 3). It was known that slugs of any size are sensitive to light and to heat [40]. Once aggregated, the cells begin a period of directed migration. Since mutant strains under dark condition showed similar slug migration distance as in the directed light and the distance of slug migration was wavelength-independent

(data not shown), it is unlikely that CBP3 is involved in light reception or signal processing (Fig. 2A, B). It is more plausible that CBP3 may be related to more general cellular locomotion machinery, which lies downstream of the signal reception site. It was known that longer slugs move more rapidly and the difference might be due to the difference in slug length [43]. But CBP3-inhibited cells showed enhanced slug migration even though it had a similar slug size with KAx3. Thus, it is reasonable that the slug trail length differences is not a secondary result of differences in aggregate size but a direct effect of the CBP3 on the cellular locomotion machinery. However, the possibility that these strains have defects in cAMP generation or processing machinery cannot be ruled out.

From the yeast two-hybrid screening using full-length CBP3 as bait, actin 8 was identified as a binding partner of CBP3. The positive interaction was also verified by two-hybrid assays, which showed a clear interaction between CBP3 and actin 8 (Fig. 4). The interaction of CBP3 and actin showed a calcium-enhanced interaction (Fig. 5A). CBP3 showed about 3-fold higher affinity toward actin in running buffer containing  $\text{Ca}^{2+}$  than EGTA. CBP3 was associated with Triton X-100-insoluble cytoskeleton and its association was increased with  $\text{Ca}^{2+}$  addition (Fig. 5B). These results demonstrated that CBP3 interacted with actin directly and  $\text{Ca}^{2+}$  enhanced this interaction.

The cellular localization of CBP3 supported the finding that CBP3 interacts with actin. CBP3 was highly enriched in the cytosolic fraction (Fig. 6D), while its main residential region was cell cortex, identical with cell cortex actin cytoskeleton (Fig. 6A, B). Also, when CBP3 was fused with green fluorescent protein and expressed in *Dictyostelium*, its localization was the same with the immunofluorescence labeling experiment (Fig. 6C). From the yeast two-hybrid assay and SPR experiment, CBP3 can bind to the monomer form of actin, G-actin, while the *in vivo* localization and detergent insoluble cytoskeleton association imply that CBP3 can bind to the filamentous form of actin, F-actin. At present, it is not clear whether CBP3 can bind G-actin or F-actin specifically. It is possible that CBP3 can bind both forms of actin with different affinity. Another possibility is that CBP3 can bind two actin molecules simultaneously and can work as a crosslinker between two F-actin filaments. Further biochemical characterization of interaction dynamics between CBP3 and actin might reveal the molecular function of CBP3 in the cytoskeleton of *Dictyostelium*.

Several actin-binding proteins have been isolated by their *in vitro* interactions with actin or searching sequence homologies in *Dictyostelium* [44]. The cellular role of these actin-binding proteins has been determined by mutant studies. Some of the mutants showed defects in phagocytosis and/or in cytokinesis [45,46] and most mutants had minor alterations in cell locomotion [47–49]. Many of these actin-binding proteins contain their own  $\text{Ca}^{2+}$ -binding sites and are regulated by  $\text{Ca}^{2+}$  [50]. From these results, it has been suggested that actin-binding proteins have redundant

functions, i.e. several proteins might share similar or overlapping functions. In this study, we found that CBP3 proteins bound actin and associated with actin cytoskeleton in a  $\text{Ca}^{2+}$ -enhanced manner and related to cell aggregation and slug migration. It was somewhat interesting that the cells overexpressing CBP3 did not show opposite effects to those under-expressing and vice-versa. For example, while the overexpressing strain led to form many smaller aggregates than parental strain, the under-expressing strain had no distinct effect on aggregation. However, in *Dictyostelium*, it has been reported that when calcium-binding protein gene was overexpressed or disrupted, they did not show opposite effects in phenotypes. The overexpression of the CAF1 has a stimulatory effect on differentiation but the CAF1-null mutant exhibited apparently normal development [18]. Like other actin-binding proteins, including CBP3, small EF-hand calcium-binding proteins may associate with certain cytoskeletal proteins and have redundant overlapping functions. This may be the reason for the subtle phenotypic changes in cells expressing different levels of CBP3. Further functional studies on these calcium-binding proteins and genetic studies involving double mutants might provide important information on the role of these proteins in *Dictyostelium*.

## Acknowledgements

We express our sincere thanks to Dr. Richard A. Firtel for the EXP-4 (+) vector, to Dr. Tom Egelhoff for the pTX-GFP vector, to Dr. Philip James for the pGBDU vector and yeast strain PJ69-4A, to Dr. Sijie Lu for *Dictyostelium* cDNA library, and to Dr. Young-Hoon Han for helpful suggestions. This work was supported by the Research Fellowship of BK21 project and Korean Research Foundation Grant (KRF-2003-041-C00318).

## References

- [1] A.K. Campbell, Intracellular calcium: its universal role as a regulator, John Wiley and Sons, New York, 1983.
- [2] D.H. O'Day (Ed.), Calcium as an intracellular messenger in eukaryotic microbes, American Society for Microbiology, Washington, DC, 1990.
- [3] I. Niki, H. Yokokura, T. Sudo, M. Kato, H. Hidaka,  $\text{Ca}^{2+}$  signaling and intracellular  $\text{Ca}^{2+}$  binding proteins, *J. Biochem. (Tokyo)* 120 (1996) 685–698.
- [4] D. Chin, A.R. Means, Calmodulin: a prototypical calcium sensor, *Trends Cell Biol.* 10 (2000) 322–328.
- [5] C.J. Weijer, Morphogenetic cell movement in *Dictyostelium*, *Semin. Cell Dev. Biol.* 10 (1999) 609–619.
- [6] D. Malchow, R. Mutzel, C. Schlatterer, On the role of calcium during chemotactic signaling and differentiation of the cellular slime mould *Dictyostelium discoideum*, *Int. J. Dev. Biol.* 40 (1996) 135–139.
- [7] S. Saran, H. Nakao, M. Tasaka, H. Iida, F.I. Tsuji, V. Nanjundiah, I. Takeuchi, Intracellular free calcium level and its response to cAMP stimulation in developing *Dictyostelium* cells transformed with jellyfish apoaequorin cDNA, *FEBS Lett.* 337 (1994) 43–47.
- [8] T. Nebl, P.R. Fisher, Intracellular  $\text{Ca}^{2+}$  signals in *Dictyostelium* chemotaxis are mediated exclusively by  $\text{Ca}^{2+}$  influx, *J. Cell. Sci.* 110 (1997) 2845–2853.
- [9] S.K. Brar, C.-H. Siu, Characterization of the cell adhesion molecule gp24 in *Dictyostelium discoideum*. Mediation of cell–cell adhesion via a  $\text{Ca}^{2+}$ -dependent mechanism, *J. Biol. Chem.* 268 (1993) 24902–24909.
- [10] A.B. Cubitt, R.A. Firtel, G. Fischer, L.F. Jaffe, A.L. Miller, Patterns of free calcium in multicellular stages of *Dictyostelium* expressing jellyfish apoaequorin, *Development* 121 (1995) 2291–2301.
- [11] Y. Kubohara, K. Okamoto, Cytoplasmic  $\text{Ca}^{2+}$  and  $\text{H}^{+}$  concentrations determine cell fate in *Dictyostelium discoideum*, *FASEB J.* 8 (1994) 869–874.
- [12] M. Azhar, P.S. Manogaran, P.K. Kennady, G. Pande, V. Nanjundiah, A  $\text{Ca}^{2+}$ -dependent early functional heterogeneity in amoebae of *Dictyostelium discoideum*, revealed by flow cytometry, *Exp. Cell Res.* 227 (1996) 344–351.
- [13] P. Schaap, T. Nebl, P.R. Fisher, A slow sustained increase in cytosolic  $\text{Ca}^{2+}$  levels mediates stalk gene induction by differentiation inducing factor in *Dictyostelium*, *EMBO J.* 15 (1996) 5177–5183.
- [14] Y. Tanaka, R. Itakura, A. Amagai, Y. Maeda, The signals for starvation response are transduced through elevated  $[\text{Ca}^{2+}]$  in *Dictyostelium* cells, *Exp. Cell Res.* 240 (1998) 340–348.
- [15] T. Liu, J.G. Williams, M. Clarke, Inducible expression of calmodulin antisense RNA in *Dictyostelium* cells inhibits the completion of cytokinesis, *Mol. Biol. Cell* 3 (1992) 1403–1413.
- [16] D. Rösel, F. Püta, A. Blahůšková, P. Smýkal, P. Folk, Molecular characterization of a calmodulin-like *Dictyostelium* protein CalB, *FEBS Lett.* 473 (2000) 323–327.
- [17] F. Abe, Y. Maeda, Specific expression of a gene encoding a novel calcium-binding protein, *CAF-1*, during transition of *Dictyostelium* cells from growth to differentiation, *Dev. Growth Differ.* 37 (1995) 39–48.
- [18] M. Itoh, M. Noguchi, Y. Maeda, Overexpression of CAF1 encoding a novel  $\text{Ca}^{2+}$ -binding protein stimulates the transition of *Dictyostelium* cells from growth to differentiation, *Dev. Growth Differ.* 40 (1998) 677–683.
- [19] B. Coukell, J. Moniakis, A. Grinberg, Cloning and expression in *Escherichia coli* of a cDNA encoding a developmentally regulated  $\text{Ca}^{2+}$ -binding protein from *Dictyostelium discoideum*, *FEBS Lett.* 362 (1995) 342–346.
- [20] A. Dharamsi, D. Tessarolo, B. Coukell, J. Pun, CBP1 associates with the *Dictyostelium* cytoskeleton and is important for normal cell aggregation under certain developmental conditions, *Exp. Cell Res.* 258 (2000) 298–309.
- [21] B. Andre, A.A. Noegel, M. Schleicher, *Dictyostelium discoideum* contains a family of calmodulin-related EF-hand proteins that are developmentally regulated, *FEBS Lett.* 382 (1996) 198–202.
- [22] Y.-H. Han, S.-O. Kang, Cloning of a cDNA encoding a new calcium-binding protein from *Dictyostelium discoideum* and its developmental regulation, *FEBS Lett.* 441 (1998) 302–306.
- [23] M. Dorywalska, B. Coukell, A. Dharamsi, Characterization and heterologous expression of cDNAs encoding two novel closely related  $\text{Ca}^{2+}$ -binding proteins in *Dictyostelium discoideum*, *Biochim. Biophys. Acta* 1496 (2000) 356–361.
- [24] M.A. Myre, D.H. O'Day, *Dictyostelium* calcium-binding protein 4a interacts with nucleomorphin, a BRCT-domain protein that regulates nuclear number, *Biochem. Biophys. Res. Commun.* 322 (2004) 665–671.
- [25] S. Fields, O. Song, A novel genetic system to detect protein–protein interactions, *Nature* 340 (1989) 245–246.
- [26] S.M. Cocucci, M. Sussman, RNA in cytoplasmic and nuclear fractions of cellular slime mold amoeba, *J. Cell Biol.* 45 (1970) 399–407.
- [27] C. Schlatterer, G. Knoll, D. Malchow, Intracellular calcium during chemotaxis of *Dictyostelium discoideum*: a new fura-2 derivative avoids sequestration of the indicator and allows long-term calcium measurements, *Eur. J. Cell Biol.* 58 (1992) 172–181.

- [28] K.M. Pang, M.A. Lynes, D.A. Knecht, Variables controlling the expression level of exogenous genes in *Dictyostelium*, *Plasmid* 41 (1999) 187–197.
- [29] P. James, J. Halladay, E.A. Craig, Genomic libraries and a host strain designed for highly efficient two-hybrid selection in yeast, *Genetics* 144 (1996) 1425–1436.
- [30] R.D. Gietz, R.H. Schiestl, Transforming yeast with DNA, *Methods Mol. Cell. Biol.* 5 (1995) 255–269.
- [31] F.M. Ausubel, R. Brent, R.E. Kingston, D.D. Moore, J.G. Seidman, J.A. Smith, K. Struhl, *Current Protocols in Molecular Biology*, Wiley, New York, 1994.
- [32] M.D. Rose, F. Winston, P. Hieter, *Methods in Yeast Genetics*, Cold Spring Harbor Laboratory Press, New York, 1990.
- [33] A. Spudich, Isolation of the actin cytoskeleton from amoeboid cells of *Dictyostelium*, *Methods Cell Biol.* 28 (1987) 209–214.
- [34] U.K. Laemmli, Cleavage of structural proteins during the assembly of the head of bacteriophage T4, *Nature* 227 (1970) 680–685.
- [35] H. Towbin, T. Staehelin, J. Gordon, Electrophoretic transfer of proteins from polyacrylamide gels to nitrocellulose sheets: procedure and some applications, *Proc. Natl. Acad. Sci. U. S. A.* 76 (1979) 4350–4354.
- [36] Y. Fukui, S. Yumura, T.K. Yumura, Agar-overlay immunofluorescence: high-resolution studies of cytoskeletal components and their changes during chemotaxis, *Methods Cell Biol.* 28 (1987) 347–356.
- [37] M. Fukuzawa, J.G. Williams, OSBPa, a predicted oxysterol binding protein of *Dictyostelium*, is required for regulated entry into culmination, *FEBS Lett.* 527 (2002) 37–42.
- [38] E. Wallraff, H.G. Wallraff, Migration and bidirectional phototaxis in *Dictyostelium discoideum* slugs lacking the actin cross-linking 120 kDa gelation factor, *J. Exp. Biol.* 200 (1997) 3213–3220.
- [39] H. Martens, J. Novotny, J. Oberstrass, T.L. Steck, P. Postlethwait, W. Nellen, RNAi in *Dictyostelium*: the role of RNA-directed RNA polymerases and double-stranded RNase, *Mol. Biol. Cell* 13 (2002) 445–453.
- [40] J.T. Bonner, A way of following individual cells in the migrating slugs of *Dictyostelium discoideum*, *Proc. Natl. Acad. Sci. U. S. A.* 95 (1998) 9355–9359.
- [41] R.J. Fisher, M. Fivash, Surface plasmon resonance based methods for measuring the kinetics and binding affinities of biomolecular interactions, *Curr. Opin. Biotechnol.* 5 (1994) 389–395.
- [42] M. Ikura, Calcium binding and conformational response in EF-hand proteins, *Trends Biochem. Sci.* 21 (1996) 14–17.
- [43] K. Inouye, I. Takeuchi, Analytical studies on migrating movement of the pseudoplasmodium of *Dictyostelium discoideum*, *Protoplasma* 99 (1979) 289–304.
- [44] A.A. Noegel, J.E. Luna, The *Dictyostelium* cytoskeleton, *Experientia* 51 (1995) 1135–1143.
- [45] J. Faix, M. Steinmetz, H. Boves, R.A. Kammerer, F. Lottspeich, U. Mintert, J. Murphy, A. Stock, U. Aebi, G. Gerisch, Corticillins, major determinants of cell shape and size, are actin-bundling proteins with a parallel coiled-coil tail, *Cell* 86 (1996) 631–642.
- [46] M. Haugwitz, A.A. Noegel, J. Karakesisoglou, M. Schleicher, *Dictyostelium* amoebae that lack G-actin-sequestering profilins show defects in F-actin content, cytokinesis, and development, *Cell* 79 (1994) 303–314.
- [47] E. Andre, M. Brink, G. Gerisch, G. Isenberg, A. Noegel, M. Schleicher, J.E. Segall, E. Wallraff, A *Dictyostelium* mutant deficient in severin, an F-actin fragmenting protein, shows normal motility and chemotaxis, *J. Cell Biol.* 108 (1989) 985–995.
- [48] A.L. Hitt, J.H. Hartwig, E.J. Luna, Ponticulin is the major high affinity link between the plasma membrane and the cortical actin network in *Dictyostelium*, *J. Cell Biol.* 126 (1994) 1433–1444.
- [49] F. Rivero, R. Furukawa, A.A. Noegel, M. Fechtmeier, *Dictyostelium discoideum* cells lacking the 34,000-dalton actin-binding protein can grow, locomote, and develop, but exhibit defects in regulation of cell structure and movement: a case of partial redundancy, *J. Cell Biol.* 135 (1996) 965–980.
- [50] M. Schleicher, A.A. Noegel, Dynamics of the *Dictyostelium* cytoskeleton during chemotaxis, *New Biol.* 4 (1992) 461–472.